Original papers
Materials for energy and environment, next-generation photovoltaics, and green technologies

УДК 544.022.537 DOI: 10.17277/jamt.2024.03.pp.188-206

Production of carbon membranes from porous polyacrylonitrile hollow fibers via IR pyrolysis

© Ala L. Yaskevich[a], Tatsiana A. Hliavitskaya[a]✉, Alexey A. Yushkin[b], Svetlana A. Pratsenko[a], Evgenii A. Nazarov[a], Mikhail N. Efimov[b], Dmitry G. Muratov[b], Tatiana V. Plisko[a], Alexandr V. Bildyukevich[a]

[a] *Institute of Physical Organic Chemistry, National Academy of Sciences of Belarus, 13, Surganov St., Minsk, 220072, Belarus,*
[b] *A.V. Topchiev Institute of Petrochemical Synthesis, Russian Academy of Sciences, 29, Leninsky Av., Moscow, 119991, Russian Federation*

✉ thliavitskaya@gmail.com

Abstract: A new approach to carbon membranes fabrication by IR pyrolysis of the hollow fiber (HF) porous membranes from a homopolymer (PAN) and acrylonitrile copolymers with methyl acrylate (PAN-MA) and itaconic acid (PAN-IA) was developed. The method includes thermal stabilization of membranes at 250 °C, and subsequent IR pyrolysis. It was established that the HF membranes made from PAN-IA and PAN were the least susceptible to destruction with increasing temperature. However, for samples based on PAN-MA, the significant deformation of hollow fiber membranes after IR pyrolysis occurs at temperatures above 200–300 °C. Scanning electron microscopy study showed that the presence of glycerol as an impregnating agent in membranes (regardless of the chemical composition of acrylonitrile copolymers) leads to a less regular and more defective structure of the resulting carbon membranes. It was found that the thermal stabilization at 250 °C preserves structural integrity and contributes to the production of mechanically stable carbon membranes. FTIR spectra confirmed that IR radiation catalyzes transformations in the polymer structure. As a result, the time of thermal stabilization and pyrolysis was noticeably reduced. It was shown, that 15 min pretreatment and 5 min pyrolysis is enough for effective stabilization of membrane structure.

Keywords: carbon membrane; homopolymer (PAN); pyrolysis; hollow fiber; copolymer; IR treatment.

For citation: Yaskevich AL, Hliavitskaya TA, Yushkin AA, Pratsenko SA, Nazarov EA, Efimov MN, Muratov DG, Plisko TV, Bildyukevich AV. Production of carbon membranes from porous polyacrylonitrile hollow fibers via IR pyrolysis. *Journal of Advanced Materials and Technologies*. 2024;9(3):188-206. DOI: 10.17277/jamt.2024.03.pp.188-206

Получение углеродных мембран из полиакрилонитрильных полых волокон методом ИК-пиролиза

© А. Л. Яскевич[a], Т. А. Глевицкая[a]✉, А. А. Юшкин[b], С. А. Праценко[a], Е. А. Назаров[a], М. Н. Ефимов[b], Д. Г. Муратов[b], Т. В. Плиско[a], А. В. Бильдюкевич[a]

[a] *Институт физико-органической химии Национальной академии наук Беларуси, ул. Сурганова, 13, Минск, 220072, Республика Беларусь,*
[b] *Институт нефтехимического синтеза им. А. В. Топчиева РАН, Ленинский пр., 29, Москва, 119991, Российская Федерация*

✉ thliavitskaya@gmail.com

Аннотация: Предложен новый подход к получению углеродных мембран при помощи ИК-пиролиза половолоконных мембран из полиакрилонитрила (ПАН) и сополимеров акрилонитрила с метилакрилатом (ПАН-МА) и итаконовой кислотой (ПАН-ИА). Предложенный способ включает термостабилизацию мембран при 250 °С и последующий ИК-пиролиз. Установлено, что половолоконные мембраны, изготовленные из ПАН-ИА

и ПАН, наименее подвержены разрушению при повышении температуры. Для образцов на основе ПАН-МА деформация половолоконных мембран в результате ИК-пиролиза регистрируется при температурах выше 200…300 °С. Исследование структуры углеродных мембран методом растровой электронной микроскопии выявило, что использование глицерина в качестве импрегнирующего агента (независимо от химического состава сополимеров акрилонитрила) приводит к менее регулярной и более дефектной структуре получаемых углеродных мембран. Установлено, что термостабилизация при 250 °С сохраняет структурную целостность и способствует получению механически стабильных углеродных мембран. Методом ИК-спектроскопии доказано, что ИК-излучение способствует существенному преобразованию структуры полимера. Показано, что 15-минутной предварительной обработки и пятиминутного пиролиза достаточно для эффективной стабилизации структуры мембраны.

Ключевые слова: углеродная мембрана; полиакрилонитрил (ПАН); пиролиз; полые волокна; сополимер; ИК-обработка.

Для цитирования: Yaskevich AL, Hliavitskaya TA, Yushkin AA, Pratsenko SA, Nazarov EA, Efimov MN, Muratov DG, Plisko TV, Bildyukevich AV. Production of carbon membranes from porous polyacrylonitrile hollow fibers via IR pyrolysis. *Journal of Advanced Materials and Technologies*. 2024;9(3):188-206. DOI: 10.17277/jamt.2024.03.pp.188-206

1. Introduction

Carbon membranes are chemical stable materials that are resistant to pressure and temperature. They are superior to traditional polymer membranes for various practical applications in gas separation, pervaporation, vapor permeation, and liquid filtration. For example, carbon membranes were used as porous cathodes for lithium batteries [1]. Carbon membranes can also act as adsorbents [2]. Due to the extremely high inner surface area (more than 1000 $m^2 \cdot g^{-1}$), such membranes can selectively absorb dissolved substances with a size of about 1 nm. The high chemical stability of carbon membranes allows for their regeneration using acidic solutions. Carbon membranes have some advantages over traditional polymer membranes for gas and vapor separation [3, 4]. Such materials are especially useful for separating olefin/paraffin mixtures or for separating natural gas (the difference in molecular diameters is at the level of 0.5 Å) [4, 5]. Carbon membranes can also be used to isolate hydrogen [6, 7] or carbon dioxide [8] from gas mixtures. Carbon membranes are also suitable for separating liquid solutions [2] and for effective separation of water–oil emulsions [9, 10]. Thus the oil rejection efficiency being over 98 % [10].

Currently, the basis for obtaining carbon membranes are polyimides [3, 4, 11], polyacrylonitrile (PAN) [2, 12, 13], phenolic resins [6, 14], polyfurfuryl alcohol [7], polyvinylidene chloride-acrylate [5], cellulose [15] and others [16, 17]. Several patents focus on the synthesis of carbon membranes [18–20]. Carbon membranes are typically produced in flat sheet or tubular membrane shapes. To obtain defect-free membranes with high mechanical strength, a dense layer of polymer was deposited on a macroporous support as a base for carbon membrane [21, 22]. During the carbonization process, the thickness of the selective layer decreased. If ceramic support was used for membrane preparation, cracking and formation of defects could occur in selective layers. Consequently, several layers were required to be deposited to eliminate all defects and obtain a defect-free membrane [23]. Flat sheet membranes can be used in plate-and-frame membrane modules, providing the membrane packing density of 300–1000 $m^2 \cdot m^{-3}$. In contrast, self-supporting membranes (tubular, capillary, hollow fiber) can significantly increase the efficiency of separation processes due to the high packing density of membranes in the module. For instance, hollow fiber membranes packing density can reach up to 30,000 $m^2 \cdot m^{-3}$ depending on the fiber diameter [22]. On the other hand, this might present challenges in providing the required mechanical strength.

At the same time, there are few reviews devoted to the production of hollow fiber carbon membranes [24–26]. Most reviews on the production of carbon fibers highlight PAN as the most common base material [27–30]. One of the reasons for this is the high degree of molecule orientation [13], due to which the pyrolysis of PAN hollow fiber membranes results in the formation of a thermally stable, highly oriented molecular structure. It provides a high mechanical strength of the resulting material. This minimizes the problem of the low mechanical strength of self-supporting carbon material. At the same time, there are also studies on the production of carbon membranes from PAN [23, 31–33]. The study of heat treatment of PAN hollow fiber membranes at 500–800 °С showed a significant effect of temperature on the pore size of the obtained carbon membrane [23]. In [31, 32] PAN-membrane modification method via heating with infrared (IR) radiation was developed. It was noted that the mechanism for forming conjugated structures in

polyacrylonitrile under the IR radiation was similar to that of the thermal transformations [34]. In this case, the structural transformations of polyacrylonitrile under IR radiation occur faster compared to traditional methods of thermal treatment [34, 35]. The IR treatment reduces the time required for insoluble structure formation without using unsafe chemicals as cross-linking agents [33, 36]. The use of IR radiation not only reduces the treatment time to several minutes, but also decreases the temperature by 50–100 °C [33]. Fabrication of PAN-membranes resistant to aprotic solvents by IR treatment consumes 6.5 times less energy compare to convective heating in a laboratory oven [36]. Carbon membranes fabricated by IR irradiation treatment exhibited more than 100 times higher productivity, with processing time and energy requirements reduced by ~20 and ~11 times, respectively, compared to a conventional electric heating method [33]. Therefore, short processing time, low power consumption, and absence of hazardous chemicals as cross-linking agents make IR-treatment an effective method for producing carbon membranes. It should be noted that the studies referenced primarily utilizws either specially synthesized PAN [31, 32] or PAN-homo-polymer [33, 36] as a precursor for carbon membrane production. While PAN-homopolymer is commonly used as a hollow fiber membrane-forming polymer, it is not the only commercially available polymer which is used for hollow fiber PAN-membranes production [37]. The introduction of comonomers (such as acrylic acid, itaconic acid, methyl acrylate and etc.) can improve certain properties of acrylonitrile polymers, such as solubility, hydrophilicity, drawability, and fiber spinning stability of hollow fibers [38]. Notably, acid comonomers such as itaconic acid are often introduced into the commercially available polymers to increase hydrophilicity; they can also reduce the cyclization temperature and improve the stabilization of the resulting carbon fiber [39, 40]. Consequently, using hollow fiber ultrafiltration membranes made from acrylonitrile copolymers as precursors for carbon membrane production is highly promising. That is why the objective of this research is to use IR pyrolysis on hollow fiber ultrafiltration membranes made from acrylonitrile polymers of various compositions to produce carbon membranes. We propose methods for producing carbon membranes by IR pyrolysis of hollow fiber ultrafiltration membranes from commercially available acrylonitrile polymers of various compositions (poly(acrylonitrile-co-methyl acrylate), poly(acrylonitrile-co-itaconic acid), PAN-homopolymer). In the process of forming membranes, it is possible to adjust the conditions for producing mechanically stable membranes. Further, during the IR pyrolysis, one can change the pore sizes in the selective layer. Using various acrylonitrile copolymers as membrane-forming polymers made it possible to study the effect of the chemical composition of acrylonitrile copolymers on the properties of the resulting carbon membranes.

2. Materials and Methods

2.1. Materials

A commercial homopolymer and two acrylonitrile copolymers were used as membrane-forming materials in this study (Table 1). Dimethylsulfoxide (DMSO, chemically pure, “Khimmed”) was used as a solvent for casting solution preparation.

Table 1. Polymers used in this study for hollow fiber membrane preparation

Sample	Polymer	Monomer unit ratio[1], %	M_w[1], kg·mol^{-1}	η_{sp}[1, 2]	Manufacturer
PAN	Polyacrylonitrile	> 99.5	200	1.64	Dolan, Germany
PAN-MA	Poly(acrylonitrile-co-methyl acrylate)	92:8	107	1.41	JSC “VNIISV”, Russia
PAN-IA	Poly(acrylonitrile-co-itaconic acid)	99:1	99	1.29	European Carbon Fibers (ECF, former EPG), Germany

[1] Data provided by the manufacturer.

[2] η_{sp} is the polymer specific viscosity.

2.2. Hollow fiber membrane preparation

Casting solutions were prepared by dissolving polymers–in DMSO, using a laboratory setup that included a thermostated stainless steel reactor and an overhead stirrer (IKARW 20 Digital, Germany). The temperature for preparation of the spinning solution was 100 °C, the preparation time was 4 hours, and the stirring speed was 800 rpm. The PAN concentration in the spinning solution was 16 wt. %.

The hollow fiber membranes were obtained by a non-solvent induced phase separation (NIPS) method using a dry-jet wet spinning process on a laboratory setup (Fig. 1). The equipment for hollow fiber membrane fabrication included a system of thermostatically controlled receiving-supply vessels and tubing for a spinning dope (*1*, Fig. 1) and an internal coagulant (*2*, Fig. 1), a stand with a spinneret assembly (*3*, Fig. 1), and a receiving tank with tap water at $T = 15$ °C (*4*, Fig. 1). The dope and the internal coagulant (water) are fed into the spinneret by compressed air, the pressure of which is controlled by pressures gauges (*5*, Fig. 1). The hollow fiber membranes are formed by gravity without winder in the system by the free-fall spinning method [41–43].

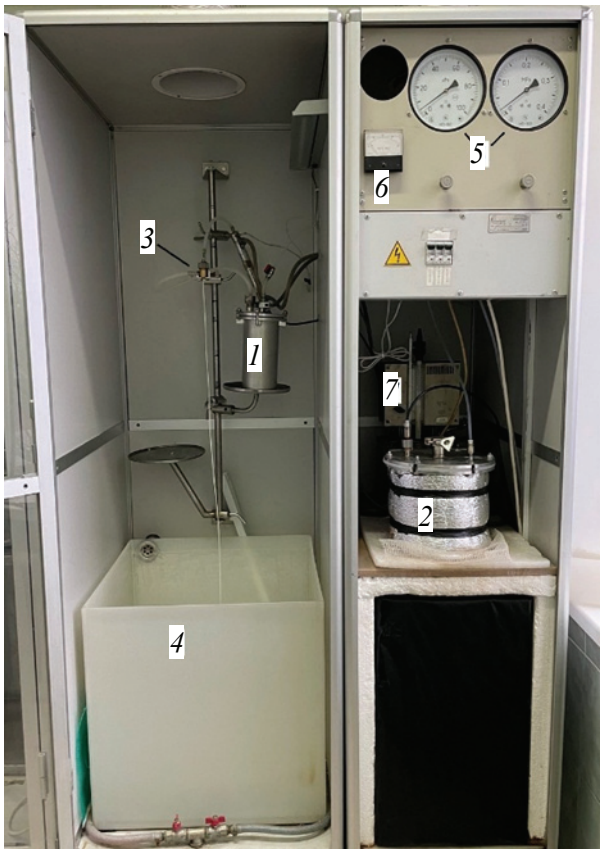

Fig. 1. Setup for the hollow fiber membrane fabrication: (*1*) spinning dope vessel; (*2*) internal coagulant bath; (*3*) spinneret; (*4*) receiving bath; (*5*) pressure gauges; (*6*) bore fluid temperature sensor and (*7*) thermostat

The hollow fibers were fabricated using various conditions: the polymer solution pressure was 200–250 kPa, the coagulant pressure was 30 kPa, the bore fluid temperature was 30 °C, and the temperature of the receiving (external coagulation) bath was 15 °C, the temperature of the polymer solutions was 40–50 °C, the air humidity was 55 %. The air gap distance was 80 cm. The outer diameter of the spinneret was 1.8 mm, the inner diameter was 0.8 mm. The spinning modes for forming PAN hollow fiber membranes were selected in accordance with the rheological behavior and properties of the polymer solution, which are given in [38].

The produced membranes were soaked in distilled water rinse bath for 12 hours to remove residual solvents and to complete the phase separation. Then, one part of the hollow fiber membranes was immersed in a 30 % glycerol aqueous solution for 24 hours and then dried for 48 hours. The other part of the membranes was dried without treatment with a glycerol solution.

2.3. Permeability of the prepared hollow fiber membranes

The permeability of individual fibers was measured on a cross-flow setup that included a gear pump (type DGS.68PPT, Tuthill Corp.) and a flow-through cell consisting of inlet and outlet capillaries and a fiber sample strung on them. Pure water flux was measured at a transmembrane pressure of 1 bar for at least 1 hour to obtain a steady-state value. The pure water flux of the membranes (J, L·m^{-2}·h) was calculated according to the equation:

$$J = \frac{V}{t\,\pi\,D_{\text{in}n}l}, \qquad (1)$$

where V is the volume of the filtrate, L; $D_{\text{in}n}$ is the inner diameter of the fiber, m; l is the fiber length, m; t is the filtration time, h.

Blue Dextran dye with a molecular weight of 70 kg·mol^{-1} was used for rejection tests. A new membrane sample was used for every rejection experiment. Before the rejection test, distilled water was filtered through a membrane for 1 hour at 1 bar. The separation test was carried out at the transmembrane pressure of 1 bar for at least 1 hour to achieve steady-state values of the rejection. All experiments were prepared with a solute concentration of 100 mg·L^{-1}. The concentration of solute in the feed and permeate was measured with a spectrophotometer at the wavelength of 620 nm. The rejection R is calculated using the relation:

$$R = \left(1 - \frac{C_p}{C_f}\right) \cdot 100\ \%, \qquad (2)$$

where C_f and C_p denote the solute concentrations in the feed and permeate respectively.

2.4. Geometric parameters and structure of the prepared membranes

The geometric dimensions of the structures of the prepared membranes were investigated by scanning electron microscopy (SEM). Two SEM microscopes were used for this purpose: Phenom Pro scanning electron microscope (Thermo Fisher Scientific, USA) with vacuum sputter coater DSR (Vaccoat, London, UK) and Phenom XL G2 Desktop SEM (Thermo Fisher Scientific, USA) with Cressington 108 auto Sputter Coater (Great Britain) table magnetron sputtering machine. Membrane transverse cleavages were obtained after preliminary membranes impregnation in isopropanol and their subsequent breaking in liquid nitrogen. A thin (5–10 nm) layer of gold was deposited on the prepared samples.

2.5. Fourier-transform infrared (FTIR) analysis

The FTIR (Nicolet Is50 spectrometer, Thermo Fisher Scientific, USA) spectra of the prepared membranes were used to investigate the chemical composition of membranes. Before measurements, the membranes were rinsed several times with distilled water and then dried for about 48 hours at room temperature.

2.6. Determination of the membranes pore size

The porosity of the membranes was determined using the POROLIQ 1000 mL instrument (POROMETER, Belgium). Membrane pore size analysis was performed by liquid-liquid displacement method [44], using water-saturated isobutanol and isobutanol-saturated water as wetting and displacement liquids, respectively. Samples of hollow fiber membranes were glued with epoxy resin into a special holder designed in such a way that both ends of the hollow fiber remained open. Three segments cut from different parts of the hollow fiber were glued into the holder. The length of the working section through which the filtration was carried out was 1 cm for each fiber. After the epoxy resin hardened, the holder with glued fibers was placed in isobutanol for 12 hours. Then the sample was placed in a measuring setup filled with a displacing liquid (aqueous phase). The excess isobutanol was removed from the sample surface due to its lower density compared to water and was subsequently removed from the setup during the measurement without affecting the process. When the holder with the membrane was placed in the setup, the transmembrane pressure increased step by step. At each pressure step, the measurement was carried out until the flow stabilized at the same level with an accuracy of ± 1 μL·min^{-1} for 180 s. The pressure was increased step by step with a step of 0.2–0.5 bar until the moment of sample breaking, which was fixed by a sharp (by 4 orders of magnitude) increase in the flow through the membrane. When the flow sensor detected such an increase in flow, the measurement automatically stopped.

The pore diameter (d_p) corresponding to a given transmembrane pressure was calculated using the Young-Laplace equation:

$$d_p = \frac{4\gamma \cos\theta}{\Delta p}, \qquad (3)$$

where γ is interfacial tension between two liquids used; θ is the contact angle between membrane and wetting liquid; Δp is transmembrane pressure.

In the used membranes, complete wetting with an alcohol-rich phase was observed, so the contact angle is 0, and $\cos\theta = 1$. The interfacial tension between the isobutanol and aqueous phases was 2.0 mN·m^{-1} at 20 °C. The main value determined for each sample was the mean flow pore size (MFP), which was determined at a pressure at which the membrane permeability was 50 % of the maximum. This value differs from the number averaged pore size upwards because it takes into account that larger pores contribute more to the overall membrane permeability.

2.7. IR-pyrolysis of hollow fibers

A laboratory IR heating furnace [33] was used for thermal stabilization and pyrolysis of hollow fiber membranes (Fig. 2). Gas line was plugged into a quartz tube with the sample and an external control unit was connected to the apparatus. If experiments were performed under a nitrogen atmosphere, the quartz tube was closed in such a way that a small hole remained at one end of the tube, and constant nitrogen flow was supplied to the tube from the opposite side. In the experiments carried out on air, the quartz tube was open from one side and the gas line was closed. The tube was surrounded by an insulating box containing IR sources. KG-220

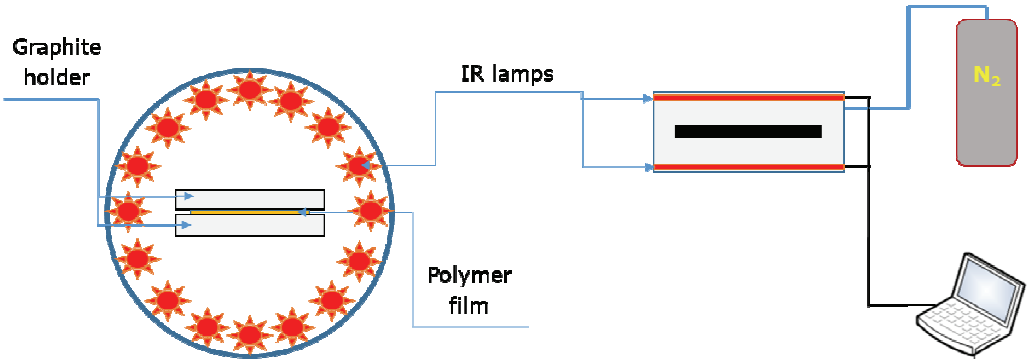

Fig. 2. Schematic illustrations of the IR furnace for membrane thermal treatment

halogen lamps with a radiation maximum in the region of 0.9–1.2 μm were used as a source of incoherent IR radiation. 3 to 6 fibers were placed in a graphite cassette for processing. During stabilization and further pyrolysis sample was freestanding without any tension. Additional quartz rods were laid between membrane samples to ensure the spatial separation of the samples without interfering with their uniform heating. The heating rate to the set temperature was 60 °C·min^{-1}. The heating rate to a given temperature varied from 5 to 60 °C·min^{-1}. The intensity of IR radiation was controlled by the heating temperature of the sample, measured using a chromel-alumel thermocouple placed directly under the sample. The control unit provided an increase and decrease in the intensity of IR radiation according to a given program. After reaching the predetermined temperature of the sample, the radiation intensity was reduced to ensure the constancy of the processing temperature for a predetermined time (1–15 minutes). Next, the IR lamps were turned off and the samples were cooled down under constant blowing with nitrogen or air.

A portion of the experiments was performed without thermal stabilization while the other part was carried out in two stages, with IR-pyrolysis preceded by thermal stabilization in air. At the end of the thermal stabilization stage, the IR lamps were turned off and the sample was allowed to slowly cool down to room temperature. Heating of the thermally stabilized samples for their pyrolysis started at room temperature.

2.8. Determination of the membrane shrinkage due to IR pyrolysis

Membrane shrinkage was calculated by the equation:

$$U = \left(1 - \frac{D_{pyr}}{D_{ref}}\right) \cdot 100\,\%, \qquad (4)$$

where U is the degree of shrinkage of hollow fiber membranes, %; D_{ref} is the outer diameter of the reference hollow fiber membrane; D_{pyr} is the outer diameter of the hollow fiber membrane after IR-pyrolysis.

2.9. Determination of the membrane strength

The strength (σ_{str}) of the resulting hollow fiber membranes was studied using a TT-1100 tensile testing machine (Cheminstruments, USA) at room temperature (25 °C). The speed of movement of the traverse was 3.8 cm/min. The samples were hollow fibers about 70 mm long, fixed between clamps. The initial distance between the clamps was 30 mm.

3. Results and Discussion

3.1. Properties of the reference hollow fiber membranes

The study of flat sheet ultrafiltration membranes formation from various acrylonitrile copolymers showed [38] that membranes prepared from acrylonitrile homopolymer solutions in DMSO with a concentration of 15 % and higher have sponge-like structures of the membrane matrix.

In this paper, hollow fiber membranes were fabricated from acrylonitrile-based polymers as precursors for carbon membranes. 16 % polymer solutions in DMSO were used for membrane preparation (Table 2). The strength of hollow fiber membranes (σ_{str}) depends on the polymer composition and drying conditions. Thus, for PAN and PAN-IA samples dried without glycerol (Sample II and Sample VI, respectively), the mechanical strength is higher than that for samples impregnated with glycerol aqueous solution before drying (Sample I and Sample V). For PAN-MA, a decrease in the mechanical strength was observed when hollow fiber membranes were dried without impregnation by glycerol (Sample IV).

Table 2. Characteristics of reference hollow fiber membranes

Sample	Polymer	Drying method	SEM	J, L·(m^{2}h)$^{-1}$	D_{ref}[1], μm	D_{int}[2], μm	L[3], μm	σ_{str}, MPa
I	PAN	Glycerol	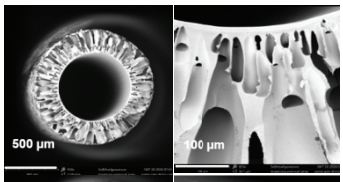	245 ± 5	1715 ± 30	1070 ± 10	320 ± 20	3.2
II	PAN	Without glycerol		185 ± 5	1750 ± 30	1095 ± 10	330 ± 20	3.6
III	PAN-MA	Glycerol	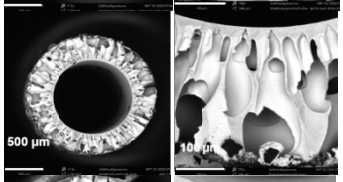	295 ± 5	1730 ± 30	1095 ± 10	310 ± 20	3.3
IV	PAN-MA	Without glycerol	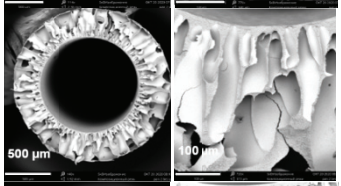	220 ± 5	1815 ± 30	1110 ± 10	330 ± 20	2.9
V	PAN-IA	Glycerol	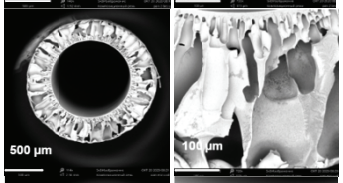	260 ± 5	1720 ± 30	1080 ± 10	320 ± 20	3.1
VI	PAN-IA	Without glycerol	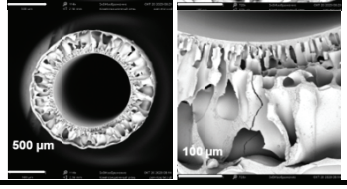	195 ± 5	1780 ± 30	1100 ± 10	330 ± 20	3.4

[1] D_{ref} is the outer diameter of the reference hollow fiber membrane.
[2] D_{int} is the fiber inner diameter.
[3] L is the fiber wall thickness.

The geometric parameters of the hollow fiber membranes dried without glycerol differ from those impregnated with glycerol: the inner diameter and the wall thickness (L) of the fibers is 20–25 and 20 μm larger, respectively. At the same time, the water permeability of hollow fiber membranes dried without glycerol is lower by 20–25 %. Thus, drying without a plasticizer (glycerol) leads to the collapse of the pores of the selective layer. Moreover, the use of a plasticizer protects the pores during drying but increases the shrinkage of the hollow fiber matrix. The increase of shrinkage is due to the increase of the mobility of polymer chains plasticized with glycerol which facilitates their rearrangement while drying.

The hollow fiber ultrafiltration membranes were produced by the method of dry-jet wet spinning, in which non-solvent-induced phase separation (NIPS) occurs. The membranes have an asymmetric structure with a thin surface selective layer (pore sizes are tens of nanometers) and a large-pore drainage layer providing mechanical strength. The drainage layer is shot through with a large number of finger-shaped vacuoles (macrovoids). Macrovoids arise from a polymer-depleted phase during NIPS membrane fabrication. The growth of macrovoids begins when the rate of diffusion of the nonsolvent in the core of the polymer-depleted phase in a freshly formed polymer film is higher than the rate of diffusion of

the solvent through the core wall. As a result, a high osmotic pressure is created, acting through the core wall, which can deform and destroy the walls of the emerging macrovoids [41]. The structure of membranes from PAN solutions in DMSO does not practically undergoes deformation after drying without glycerol (see scanning electron microscopy (SEM) results) in contrast to the structure of PAN-MA membrane samples (Table 2). In the case of membrane samples from the PAN-IA copolymer, the formation of a finer porous structure is observed. On the other hand, the membranes from the PAN-MA copolymer were partially deformed after drying without glycerol.

3.2. Change in characteristics of hollow fiber membranes after IR pyrolysis

In this section, one-stage pyrolysis without thermal stabilization was used for carbon membrane preparation. The heating rate was 50 °C·min^{-1}, and the pyrolysis time at the maximum processing temperature was 2 minutes. As studies of the prepared carbon membranes showed, shrinkage of hollow fibers occurs as a result of IR pyrolysis. The degree of shrinkage depends on the chemical nature of the membrane-forming polymer and drying conditions (with or without glycerol) (Fig. 3). Measurement of hollow fiber membranes dimensions after pyrolysis showed that in the temperature range from 200 to 500 °C there is a significant decrease in the linear dimensions (diameter, length) of the membranes, reaching 62 % (Fig. 3). Such significant decrease in linear dimensions (diameter, length) may be associated with shrinkage which stemmed from the evolving gases (as a result of membrane burn off) [45] With a further increase in temperature, almost no changes in the dimensions of the samples were observed. All samples was brittle and not flexible but their strength was enough for further processing.

The comparison of different copolymers shows that the smallest shrinkage was observed in the case of PAN-IA membranes (40–50 %) (Fig. 3*c*). The membranes obtained from PAN slightly exceeded them in terms of shrinkage (45–52 %) (Fig. 3*a*), while the samples from PAN-MA lost more in size (52–62 %) (Fig. 3*b*). In addition, samples from PAN-IA were more resistant to cracking during the pyrolysis.

Differences were also observed in the structures of carbon membranes (Fig. 4). After IR pyrolysis of hollow fiber membranes dried without glycerol, the structure of the resulting carbon membranes was more regular and less defective, with a non-porous inner layer compared to hollow fiber membranes dries with glycerol. For carbon membranes made from PAN-MA (Samples III and IV), a more pronounced deformation of the membrane matrix was observed, which explains the results obtained on fiber shrinkage (Fig. 3*b*). The structures of carbon membranes obtained from PAN hollow fiber membranes impregnated with glycerol (Sample I) and those without glycerol (Sample II) differ slightly, although the shrinkage of the fibers after drying with glycerol was higher (Fig. 3*a*). For carbon membranes based on samples of hollow fiber membranes from PAN-MA and PAN-IA dried with glycerol, there are areas with an inhomogeneous structure and remnants of the porous structure of the membranes (Fig. 4, Sample III and Simple V, respectively). This may be due to several reasons: (1) during the IR pyrolysis some of the energy was wasted on glycerol evaporation; (2) plasticized polymer chains featured

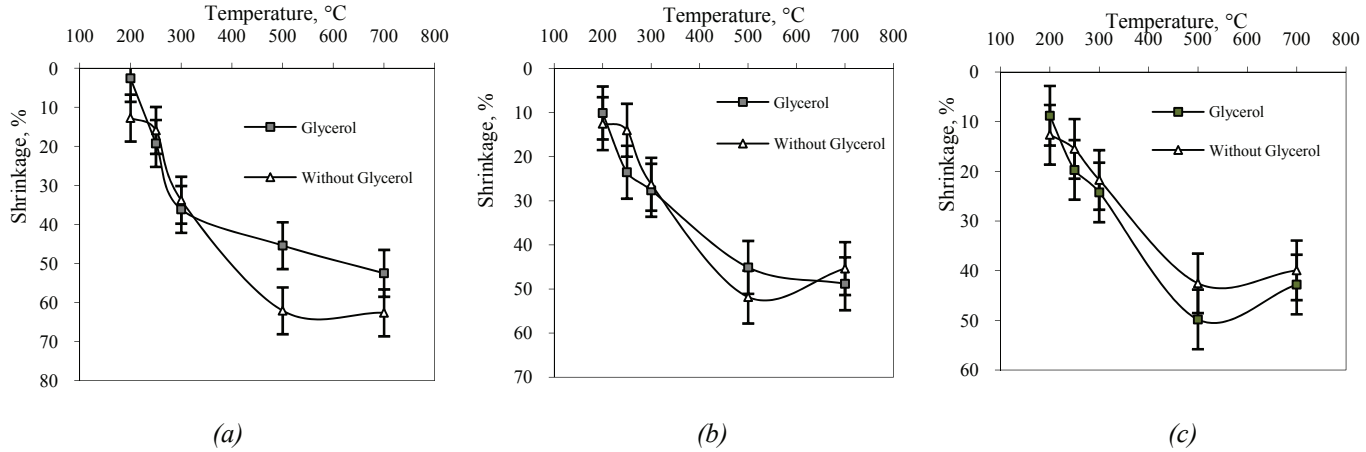

Fig. 3. Shrinkage of hollow fiber membranes depending on the IR pyrolysis temperature:
a – PAN; *b* – PAN-MA; *c* – PAN-IA

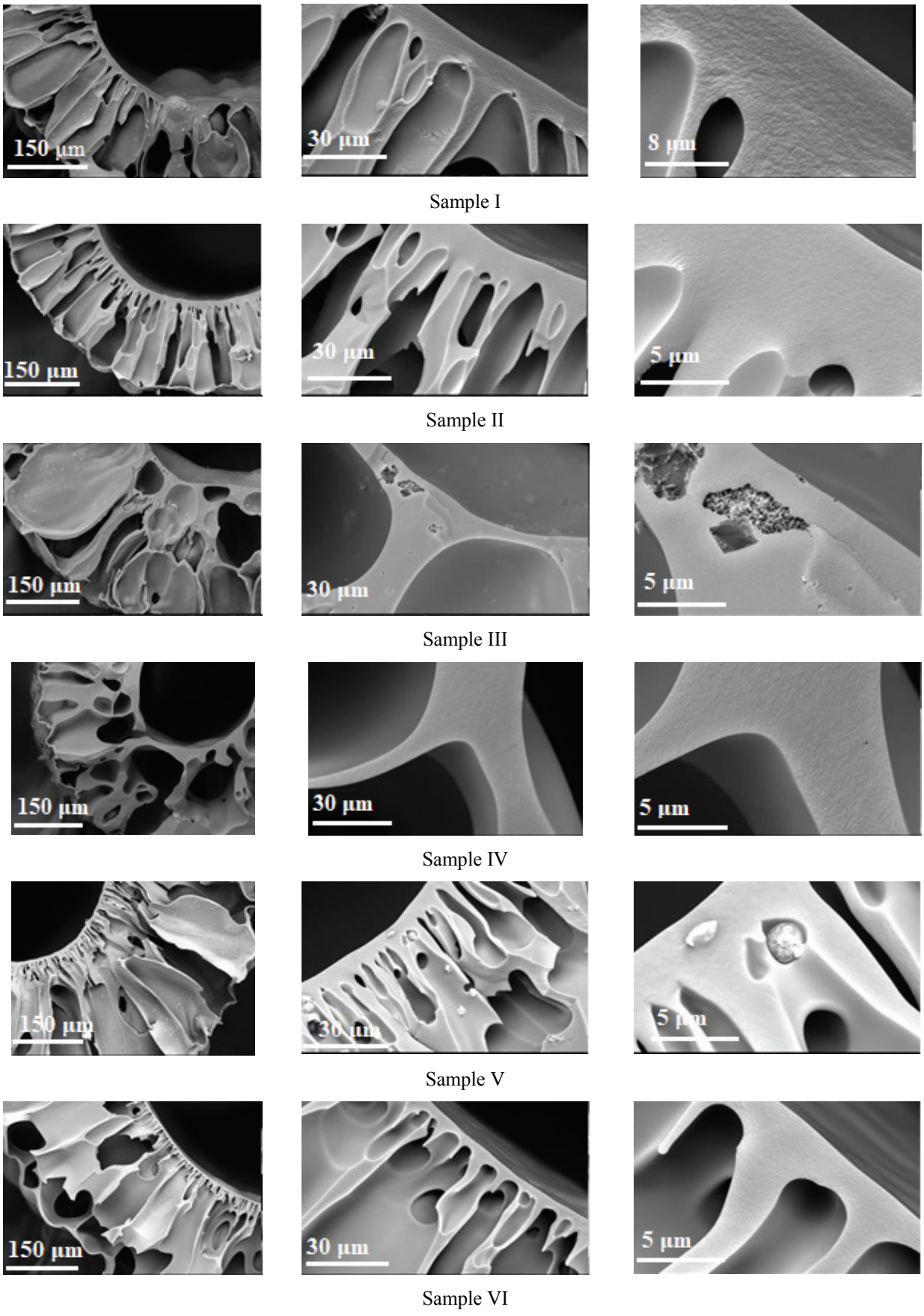

Fig. 4. SEM images of hollow fiber membranes after IR pyrolysis at 700 °C

Fig. 5. PAN hollow fiber membranes (Sample I) after pyrolysis in nitrogen atmosphere at different temperatures

increased mobility and can be rearranged during IR pyrolysis; (3) glycerol can impregnate membrane pore structure non-uniformly since membrane lumen is less accessible for glycerol penetration.

A study of the structure of membranes prepared at different temperatures showed that up to a temperature of 400 °C, no noticeable changes were observed in the structure of membrane cross-section. However, for membranes pyrolyzed at temperatures of 400 °C and higher, the structure of the membranes turned out to be significantly deformed (Fig. 4 and 5). It was found that the changes that occur during pyrolysis also depend on the material used and the drying method (with or without glycerol). The degree of deformation was bigger on the outer surface of the samples, while the inner layer as a whole remained unchanged. The observed deformations, most likely, resulted from the shrinkage of the samples during annealing.

A study of the mechanical strength of hollow fiber membranes after IR pyrolysis showed (Table 3) that at a treatment temperature of 200 °C, the strength of carbon membranes decreased by 20–24 % compared to the reference membranes (Table 2). With a further increase in temperature to 500 °C, the strength of the membranes decreased by more than 50 %. An increase in temperature above 500 °C did not lead to a further decrease in strength. The comparison of samples initially dried without glycerol (IV) and dried after impregnation with glycerin solution (I and V) showed that the strength of hollow fibers after IR pyrolysis was practically independent of the drying method and polymer composition.

Table 3. Strength of membranes at different temperature IR pyrolysis in nitrogen atmosphere

IR-pyrolysis temperature, °C	σ_{str}, MPa		
	Sample I	Sample IV	Sample V
200	2.5	2.3	2.4
250	2.1	2.0	2.1
300	1.9	1.8	1.9
400	1.6	1.4	1.5
500	1.3	1.1	1.2
600	1.3	1.0	1.1
700	1.2	1.1	1.2

Table 4. Characteristics of hollow fiber membrane samples after IR pyrolysis in nitrogen atmosphere at different temperatures

Sample	Pore size, nm			Rupture pressure, bar			
	Initial	200 °C	250 °C	Initial	200 °C	250 °C	300 °C
I	27.5	~7.5	<5.8	6.0	>11	>14	10.1
II	11.7	9.9	3.8	7.0	8.3	23.1	14.2
III	38.1	7.9	4.1	6.9	>10.5	>20	16.4
IV	10.4	<7.2	<7.2	8.0	>11	>11	14.1
V	27.6	12.3	7.0	5.5	9.9	13.0	11.0
VI	13.6	~7.8	4.1	6.6	15.3	19.7	14.7

Porosimetric studies of membranes before and after IR pyrolysis showed that the main decrease in membrane pore size was observed in the pyrolysis temperature range of 200–300 °C (Table 4). For membrane samples impregnated with glycerol (I, III, V), the pore sizes were 2–3 times higher than the pore sizes of membranes dried without glycerol (II, IV, VI). After IR pyrolysis at 200 °C, the pore sizes of membrane samples I, III, and V decreased to 7.5–12 nm and were comparable with the pore sizes of membrane samples II, IV, and VI. After IR pyrolysis at 250°C, the pore sizes of the samples decreased to 3.8–7.2 nm. For samples subjected to IR pyrolysis at a higher temperature, the pore size could not be determined due to the necessity of using high pressures that exceed the limiting pressure that the membranes were able to withstand.

A study of the tensile strength of the membrane samples showed (Table 4) that the rupture pressure of the hollow fibers increased after IR pyrolysis at 200 °C for all samples. With an increase in temperature to 250 °C, the rupture pressure of the samples also increased. However, with an increase in temperature up to 300 °C, the fiber rupture pressure for most samples decreased.

The obtained results indicate that during the IR pyrolysis of samples in a nitrogen atmosphere at temperatures of 200–300 °C, membrane shrinkage is accompanied by decrease in transport pore size in the selective layer of membranes. At the same time, at temperatures above 400 °C, although the main structure of the membrane remains unchanged, liquid porosimetry results indicate that most of the transport pores have already collapsed. Further sample shrinkage leads to deformation of the membrane macrostructure.

Testing of membranes from various PAN copolymers revealed that PAN-IA membranes experience less shrinkage during pyrolysis and are less susceptible to cracking, which makes this polymer optimal for carbon membrane preparation.

3.3. Influence of preliminary thermal stabilization on the membrane characteristics

As it was shown in Fig. 3, the geometric parameters of hollow fibers were changed with an increase in the temperature of IR pyrolysis. The study of the carbon membranes obtained with and without thermal stabilization using SEM showed that the samples subjected to IR pyrolysis after thermal stabilization demonstrated absence of structure deformations with an increase in the pyrolysis temperature (Table 5). In the absence of thermal stabilization, the structure of hollow fiber membranes after IR pyrolysis is significantly deformed. The destruction of the structure is especially noticeable for hollow fiber membranes impregnated with glycerol, apparently due to a more significant decrease in the pore size during pyrolysis.

The PAN-IA membranes were least susceptible to degradation with increasing temperature after IR treatment with thermal stabilization. Membranes dried without glycerol (Table 5, Sample VI), even at high temperatures of IR pyrolysis, preserved their geometrically regular structures. In contrast, glycerol-impregnated membranes (Table 5, Sample V) demonstrated a greater deformation of the structure after a one-stage IR pyrolysis. A similar trend was observed with the PAN samples (Table 5, Sample II). Similar to PAN-IA samples, PAN-membranes retained their structure after IR pyrolysis with thermal stabilization. However, without thermal stabilization membranes impregnated with glycerol experienced a significant deformation at a temperature of 500 °C and above (Table 5, Sample I). For PAN-MA-based samples (Table 5, Samples III and IV) structural changes after IR pyrolysis with thermal stabilization were comparable to those of PAN-IA and PAN samples. However, after IR pyrolysis without thermal stabilization, the deformation of hollow fiber membranes was notably significant at temperatures above 200–300 °C. Such significant deformation of

Table 5. SEM cross-section of membranes from PAN after IR-pyrolysis in various ways

Sample	Thermal stabilization (250 °C) and IR pyrolysis *T*, °C			IR pyrolysis *T*, °C		
I	300	500	700	300	500	700
	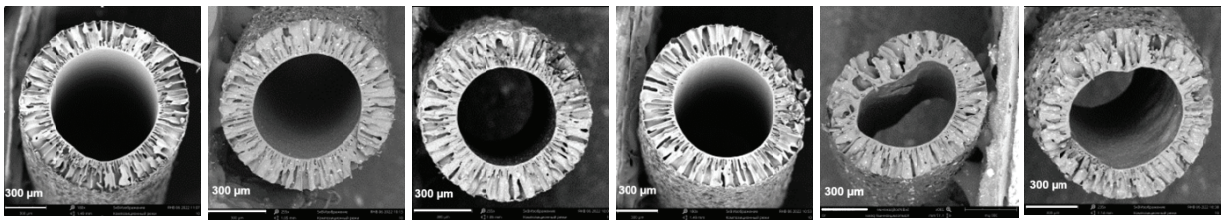					
II	300	500	700	300	600	700
	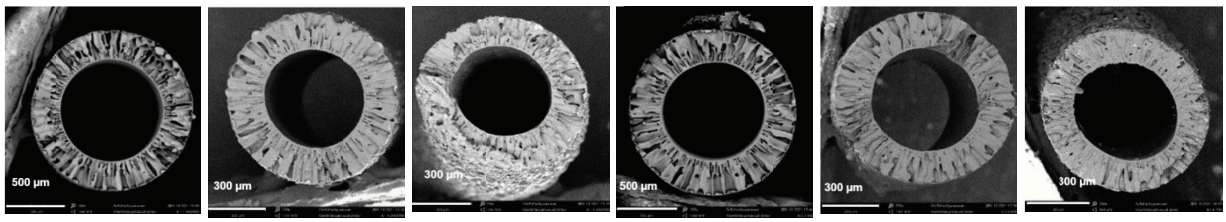					
III	300	500	700	200	500	700
	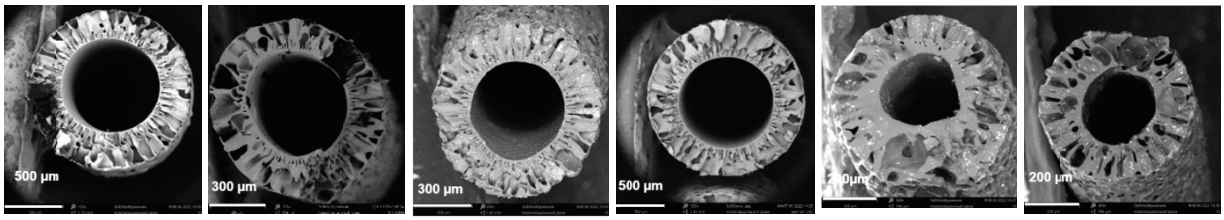					
IV	300	400	700	300	400	700
	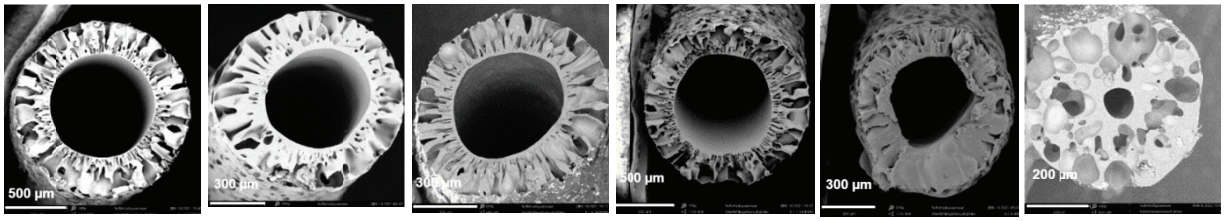					
V	300	400	600	300	400	600
	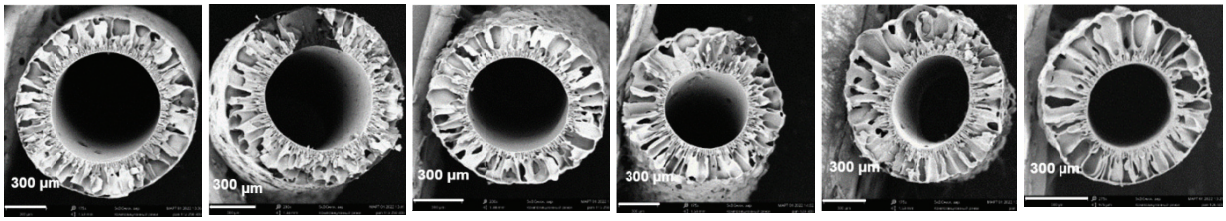					
VI	300	500	700	300	500	700
	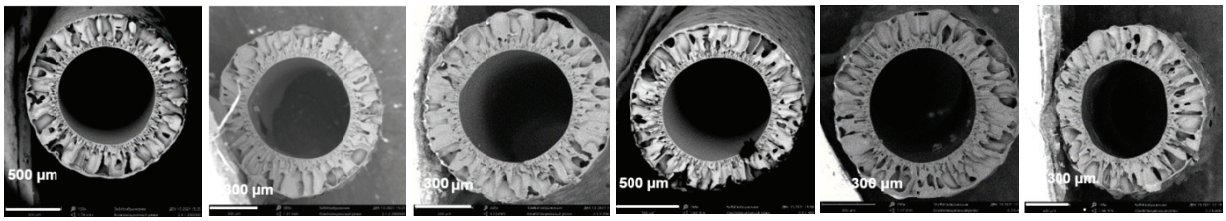					

glycerol impregnated membrane structure is likely due to an extreme reduction in the pore size resulting from the IR treatment. Impregnation of ultrafiltration membranes with glycerin solution is carried out to prevent pore contraction and is responsible for the high membrane flux [46]. This aligns well with the data presented in Table 4. Initial membranes impregnated with glycerol have pore sizes 2.0–3.6 times higher than those of initial membranes without glycerol. It is worth noting that other alcohols, such as isopropanol, ethanol, etc. can also be used as impregnating agents [47].

Using FTIR spectroscopy of prepared carbon membranes, a change in the chemical composition of samples after IR pyrolysis was investigated (Fig. 6). As the pyrolysis temperature increased from 200 to 400 °C, a decrease in the number of methylene groups (~2850, 2930, 1450 cm^{-1}) was observed. At temperatures of 400 °C and above the nitrile (~2250 cm^{-1}) and carbonyl (~1730 cm^{-1}) groups disappeared likely due to the initiation of the cyclization reaction [48]. At 400–500 °C a sharp peak was detected at 1590 cm^{-1}, representing a mix of C=N, C=C and C–N bonds [30]. This peak indicates the formation of cyclic structure of molecular chains, specifically through conversion of CN to C=N by cyclization [49]. The appearance of the C=C group was due to the dehydrogenation reaction [40]. The results of FTIR spectroscopy did not reveal significant differences in the resulting structures. The transformed peak shapes were nearly identical for all precursors. Carbonization of the samples apparently occurs at temperatures of 600–700 °C. At these temperatures FTIR spectra of membranes become flatter and the characteristic peaks rather diminish. The absence of these peaks indicates that PAN is completely converted to the cyclic carbon structure. Notably, compared to the FTIR spectrum of PAN-membranes, FTIR spectrum of the initial PAN-IA membrane had a characteristic band at 1710 cm^{-1} corresponding to C=O bond of itaconic acid. In the case of PAN-IA, cyclization and dehydrogenation were facilitated by itaconic acid through an ionic mechanism. Conversely, in the case of homopolymer, the cyclization of nitrile groups was initiated only through a free radical mechanism. The cyclization mechanisms were described in more detail in [30, 40].

In the FTIR spectra of carbon membranes based on hollow fibers dried without glycerol, a band ~1600–1590 cm^{-1} (C=N) appears after IR pyrolysis at 300 °C (Fig. 6). A sharp disappearance of nitrile groups and a shift of the C=N bond band to 1570 cm^{-1} after pyrolysis at 400 °C was observed. At the same time, there were no significant differences in the spectra of the samples after IR pyrolysis with and without thermal stabilization. The spectra of samples obtained by IR pyrolysis with thermal stabilization were almost identical to the spectra of carbon membranes based on hollow fibers dried without glycerol. In the case of IR pyrolysis without thermal stabilization at 300–400 °C, a significant increase in the intensity of mix of C=N, C=C and C–N bonds at 1590 cm^{-1} was noted for PAN-MA and PAN-IA copolymers. This is due to the fact that the presence of a partially ionic structure eases the cyclization process [45].

3.4. Optimization of thermal stabilization conditions

The membranes subjected to thermal stabilization at a temperature of 200–240 °C for 15 minutes were more prone to deformation and cracking during pyrolysis (500°C, 2 minutes) (Fig. 7). According to the FTIR spectra in Figs. 4 and 5, the pyrolysis at 500 °C has not finished the carbonization; therefore, higher temperature (600–700 °C) can be used during pyrolysis of the hollow fiber membranes. However, since the carbon membranes being developed are planned to be used for both gas separation and nanofiltration, it was decided to limit the pyrolysis temperature to 500 °C. This decision aligns with the data in [13], since at a very high temperature the pore size of membranes starts to decrease, ultimately leading to collapse.

Membranes, which underwent thermal stabilization at a temperature of 260–300 °C, retained its integrity. Further experiments in narrower temperature interval 240–260 °C showed that optimal temperature of thermal stabilization was 250 °C. At this temperature of thermal stabilization, the subsequent pyrolysis did not result in undesirable phenomena of cracking or deformation of the membranes. This suggests that heating of the sample under IR conditions follows similar mechanisms to traditional convectional heating. Hence, thermal stabilization in an oxygen-containing atmosphere is important for maintaining membrane integrity during further pyrolysis at temperatures above 300 °C. At the same time, IR irradiation intensifies ongoing reactions, decreasing the time needed to achieve the desired conversion.

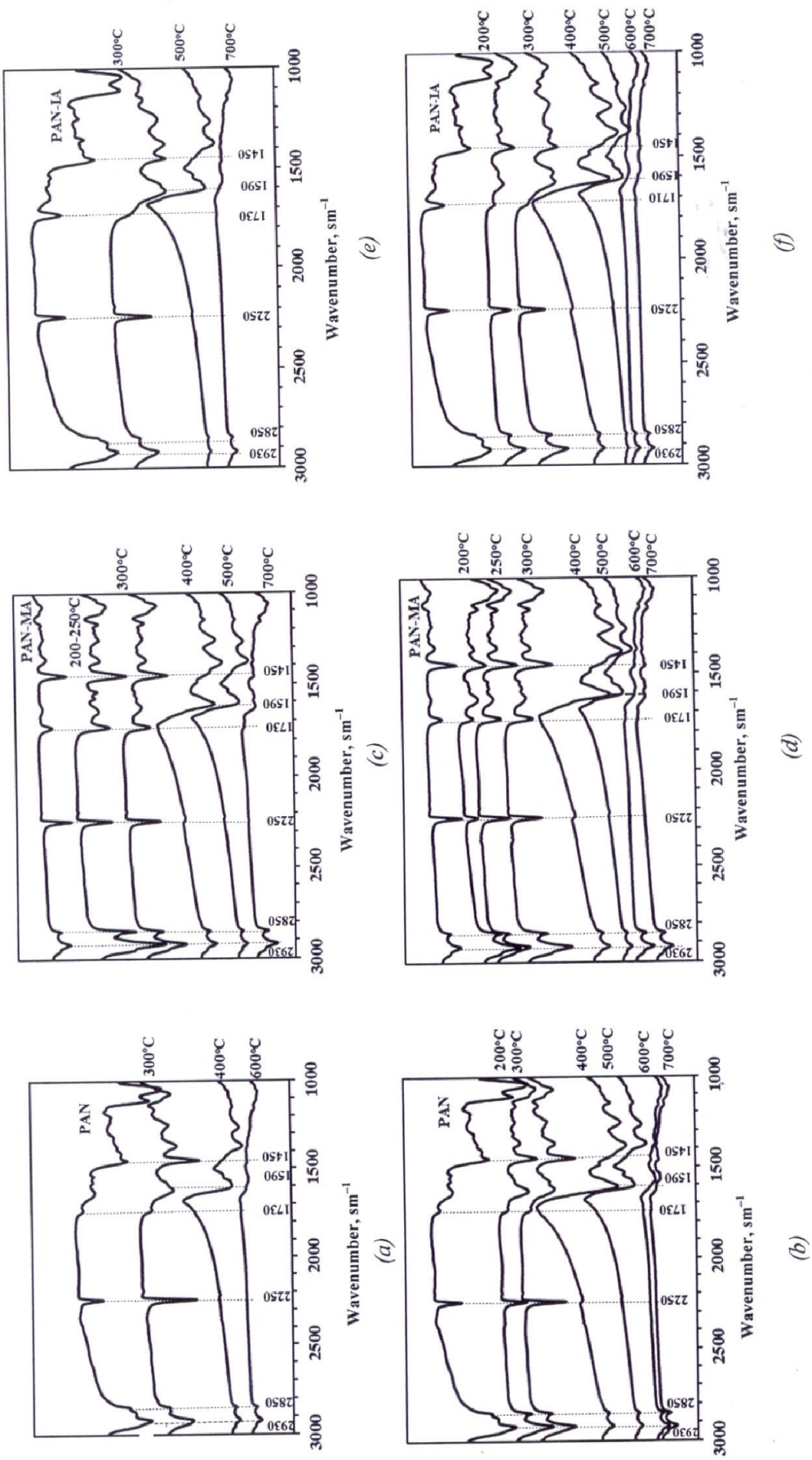

Fig. 6. FTIR of carbon membranes from Sample II (*a*, *b*), Sample IV (*c*, *d*) and Sample VI (*e*,*f*).
Processing conditions: *a*, *c*, *e* – thermal stabilization at 250 °C and IR pyrolysis; *b*, *d*, *f* – IR pyrolysis

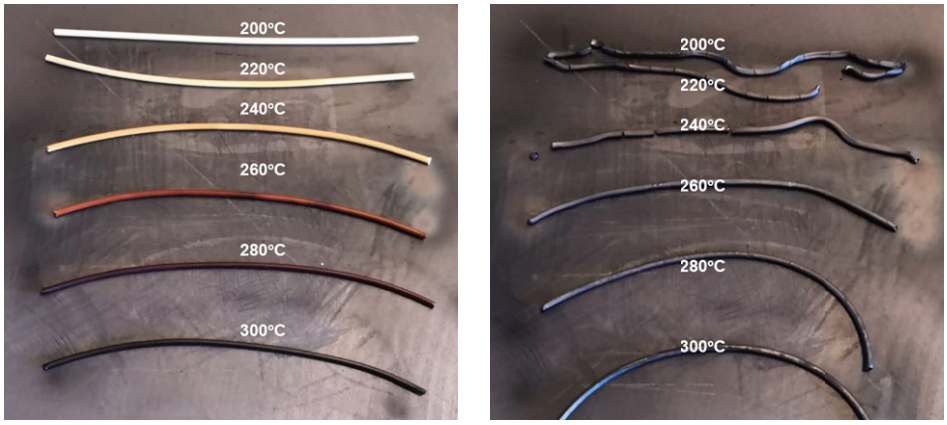

(a) *(b)*

Fig. 7. Hollow fiber membranes after thermal stabilization (15 minutes) at various temperatures, before (*a*) and after (*b*) the pyrolysis stage at a temperature of 500 °C (2 minutes)

A similar behavior was observed when varying the thermal stabilization time. The membranes subjected to thermal stabilization (250 °C) for 5–10 minutes cracked during subsequent pyrolysis (500 °C, 2 minutes), while at a longer thermal stabilization time, the membranes retained their integrity. It is noteworthy that as the thermal stabilization time increased from 5 to 15 minutes, the color of membranes changed from pale beige to brown. With a further increase in the process time, no further changes in the membrane were observed. The thermal stabilization process required only 15 minutes, which is less than the time needed for thermal stabilization through convectional heating methods.

The obtained results also show that optimal thermal stabilization degree can be achieved at lower temperatures by increasing the treatment time.

The study investigated the influence of the heating rate of hollow fiber membranes by IR radiation during thermal stabilization and subsequent pyrolysis in the range of 5–60 °C·min^{-1}. The thermal stabilization parameters corresponded to the previously determined optimal values – 250 °C for 15 minutes, pyrolysis – 500 °C for 2 minutes. By varying the heating rate during thermal stabilization, it was found that at a low heating rate of 5 and 10 °C·min^{-1}, the samples retained their integrity during the subsequent pyrolysis; however, at higher heating rates, the pyrolysis of hollow fiber membranes led to their cracking. During pyrolysis, the heating rate was fixed at 60 °C·min^{-1}. The reason for this is that an increase in the heating rate leads to a decrease in the total processing time. This resulted in an insufficient level of sample stabilization before the pyrolysis stage. Thus, the value of 10 °C·min^{-1} was chosen as the optimal heating rate, at which a sufficient level of thermal stabilization of the membrane before IR pyrolysis is achieved.

The pyrolysis time at the maximum temperature ranged from 1 to 15 minutes. The membranes retained their integrity over the entire range of times. However, as the pyrolysis time exceeded 2 minutes, the strength of the membranes deteriorated. The drop of membrane strength was low, with a reduction not exceeding 10 % at maximum processing time.

The study of the influence of the heating rate during the pyrolysis process yielded similar finidngs: during the pyrolysis process, the membranes retained their integrity across all tested heating rates. All samples exhibited brittleness and poor flexibility after thermal stabilization and pyrolysis. No difference in membrane integrity was observed during the pyrolysis process with different heating rates, indicating that shorter processing time is preferable for the pyrolysis process. This contrasts with traditional convective heating, where lower heating rates are preferable to prevent membrane destruction. In IR processing reactions occur faster, making it possible to obtain membranes with shorter processing times. Hence, 60 °C·min^{-1} and 2 minutes were chosen as the optimal heating rate and time for the pyrolysis stage.

3.5. Filtration performance of obtained membranes

Filtration performances were measured for membranes annealed at different IR treatment temperatures ranging from 200 to 500 °C. For membranes annealed at 200 and 250 °C, preliminary thermal stabilization was not applied. In contrast, for higher temperatures, thermal stabilization in air was applied for 15 minutes at a maximum temperature of 250 °C. The heating rate at

Table 6. Pure water flux and Blue Dextran rejection for hollow fiber membranes after different temperatures of IR treatment

IR treatment temperature, °C	Sample I		Sample IV		Sample V	
	J, L·(m^2·h)$^{-1}$	R, %	J, L·(m^2·h)$^{-1}$	R, %	J, L·(m^2·h)$^{-1}$	R, %
200	160	38	199	48	187	29
250	60	>99	68	95	62	68
300	18.7	>99	19.9	>99	19.0	99
400	10.5	>99	11.8	>99	11.5	>99
500	5.2	>99	6.7	>99	5.6	>99

thermal stabilization stage was 10 °C. After the thermal stabilization stage, the samples were subjected to pyrolysis in nitrogen atmosphere at a given temperature for 2 minutes. The heating rate in the pyrolysis process was 60 °C.

The pure water flux through membranes treated at a temperature of 200 °C was 10–15 % lower than that for the initial ones (160–199 L·(m^2·h)$^{-1}$ compared to 187–234 L·(m^2·h)$^{-1}$) (Table 6). At a temperature of 300 °C, the flux dropped by an order of magnitude to 18.7–19.9 L·(m^2·h)$^{-1}$. A further increase in temperature to 500 °C led to a decrease in pure water flux to 5.2–6.7 L·(m^2·h)$^{-1}$. At the same time, the membranes retained more than 99 % of the Blue Dextran dye with a molecular weight of 70 kg·mol^{-1} (Table 6), which indicates that the obtained membranes were defect-free.

The decrease in pure water flux with an increasing IR treatment temperature was due to a decrease in pore size. Although the pore radius was not measured because of the high pressure needed for measuring such small pores, from filtration performances and shrinkage data (Fig. 3) it can be concluded that further decrease in pore size took place with increase of IR pyrolysis temperature. At the same time, complete collapse of the pores does not occur. From the other hand, high Blue Dextran rejection confirms absence of membrane cracking and appearance of defects during pyrolysis.

The obtained results demonstrated that IR irradiation can be used for preparation of carbon hollow fiber membranes. At the same time, by regulating the pyrolysis temperature it is possible to control the pore size of the obtained porous membranes.

4. Conclusion

A new technique for obtaining carbon membranes using IR radiation for heating the hollow fiber membranes has been developed. The optimal conditions for IR pyrolysis have been determined. It was found that in the case of IR heating, samples of PAN hollow fiber membranes must be thermally stabilized in air at a maximum temperature of 250 °C for at least 15 minutes. Thermal stabilization is a necessary step in membrane processing, similar to convectional heating. It makes it possible to avoid undesirable effects of destruction and deformation of membranes during pyrolysis. Following the thermal stabilization stage, the samples are subjected to pyrolysis in an inert atmosphere. An optimal heating rate of 60 °C·min^{-1} for duration of 2 minutes was chosen for the pyrolysis stage. The short processing time and high heating rate is preferable for pyrolysis process. This distinguishes IR heating from traditional convective heating. In the latter case, the lower heating rate is preferable to prevent membrane destruction. Faster processes associated with IR processing make it possible to obtain membranes with reduced processing time.

It has been established that IR pyrolysis of hollow fiber membranes prepared by spinning from 16 % solutions of PAN, PAN-MA, and PAN-IA in DMSO results in shrinkage of hollow fibers with the degree of shrinkage depending on the chemical nature of the membrane-forming polymer and drying conditions. The structure of the resulting carbon membranes was more regular and less defective if the porous membrane was not impregnated with glycerol. The PAN-MA samples were more prone to shrinkage and deformation of the membrane matrix, while PAN-IA samples demonstrated less shrinkage. The appearance of samples subjected to IR pyrolysis after thermal stabilization at 250°C significantly improved, practically no deformation of the structure was observed at higher pyrolysis temperatures. Without thermal stabilization, the structure of hollow fiber membranes after IR pyrolysis demonstrated significant deformation, particularly noticeable in hollow fibers impregnated with glycerol, apparently due to a more significant decrease in the pore size during pyrolysis.

5. Funding

This work was supported by Russian Foundation for Basic Research, Russian Federation (project number 20-58-00033 Bel_a) and Belarusian Republican Foundation for Fundamental Research, Belarus (project number X20P-185).

6. Acknowledgements

The authors express gratitude to D. Bakhtin for SEM images. This research was performed using the equipment of the Shared Research Center "Analytical center of deep oil processing and petrochemistry of TIPS RAS".

7. Conflict of interests

The authors declare no conflict of interest.

References

1. Choudhury S, Fischer D, Formanek P, Simon F, et al. Porous carbon prepared from polyacrylonitrile for lithium-sulfur battery cathodes using phase inversion technique. *Polymer*. 2018;151:171-178. DOI:10.1016/j.polymer.2018.07.026

2. Wu Q, Liang H, Li M, Liu B, et al. Hierarchically porous carbon membranes derived from pan and their selective adsorption of organic dyes. *Chinese Journal of Polymer Science*. 2016;34(1):23-33. DOI:10.1007/s10118-016-1723-6

3. Adams JS, Itta AK, Zhang C, Wenz GB, et al. New insights into structural evolution in carbon molecular sieve membranes during pyrolysis. *Carbon*. 2019;141:238-246. DOI:10.1016/j.carbon.2018.09.039

4. Chu Y-H, Yancey D, Xu L, Martinez M, et al. Iron-containing carbon molecular sieve membranes for advanced olefin/paraffin separations. *Journal of Membrane Science*. 2018;548:609-620. DOI:10.1016/j.memsci.2017.11.052

5. Liu J, Calverley EM, McAdon MH, Goss JM, et al. New carbon molecular sieves for propylene/propane separation with high working capacity and separation factor. *Carbon*. 2017;123:273-282. DOI:10.1016/j.carbon.2017.07.068

6. Roy S, Das R, Gagrai MK, Sarkar S. Preparation of carbon molecular sieve membrane derived from phenolic resin over macroporous clay-alumina based support for hydrogen separation. *Journal of Porous Materials*. 2016;23(6):1653-1662. DOI:10.1007/s10934-016-0226-8

7. Xu S, Lin X, He Y, Wang Z, et al. Carbon membrane performance on hydrogen separation in H_2H_2O HI gaseous mixture system in the sulfur-iodine thermochemical cycle. *International Journal of Hydrogen Energy*. 2017;42(6):3708-3715. DOI:10.1016/j.ijhydene.2016.08.101

8. He X, Hägg M-B. Hollow fiber carbon membranes: investigations for CO_2 capture. *Journal of Membrane Science*. 2011;378(1-2):1-9. DOI:10.1016/j.memsci.2010.10.070

9. Du L, Quan X, Fan X, Chen S, et al. Electro-responsive carbon membranes with reversible superhydrophobicity/superhydrophilicity switch for efficient oil/water separation. *Separation and Purification Technology*. 2019;210:891-899. DOI:10.1016/j.seppur.2018.05.032

10. Pan Y, Wang W, Wang T, Yao P. Fabrication of carbon membrane and microfiltration of oil-in-water emulsion: an investigation on fouling mechanisms. *Separation and Purification Technology*. 2007;57(2):388-393. DOI:10.1016/j.seppur.2007.04.024

11. Fu S, Sanders ES, Kulkarni SS, Wenz GB, et al. Temperature dependence of gas transport and sorption in carbon molecular sieve membranes derived from four 6FDA based polyimides: entropic selectivity evaluation. *Carbon*. 2015;95:995-1006. DOI:10.1016/j.carbon.2015.09.005

12. Lee HS, Baek GY, Jeong SY, Shin K, et al. Preparation of thin porous carbon membranes from polyacrylonitrile by phase separation and heat treatment. *Journal of Nanoscience and Nanotechnology*. 2017;17(8):5822-5825. DOI:10.1166/jnn.2017.14135

13. Development and characterization of polyacrylonitrile(PAN) based carbon hollow fiber membrane. Available from: https://www.semanticscholar.org [Accessed 29 April 2024]

14. Rodrigues SC, Whitley R, Mendes A. Preparation and characterization of carbon molecular sieve membranes based on resorcinol-formaldehyde resin. *Journal of Membrane Science*. 2014;459:207-216. DOI:10.1016/j.memsci.2014.02.013

15. He X, Lie JA, Sheridan E, Hägg M-B. Preparation and characterization of hollow fiber carbon membranes from cellulose acetate precursors. *Industrial & Engineering Chemistry Research*. 2011;50(4):2080-2087. DOI:10.1021/ie101978q

16. Ma X, Swaidan R, Teng B, Tan H, et al. Carbon molecular sieve gas separation membranes based on an intrinsically microporous polyimide precursor. *Carbon*. 2013;62:88-96. DOI:10.1016/j.carbon.2013.05.057

17. Park HB, Lee SY, Lee YM. Pyrolytic carbon membranes containing silica: morphological approach on gas transport behavior. *Journal of Molecular Structure*. 2005;739(1-3):179-190. DOI:10.1016/j.molstruc.2004.08.028

18. Tena A, Rangou S, Shishatskiy S. *Method of producing a thermally rearranged PBX, thermally rearranged PBX and membrane*. United States patent 10,301,431. 28 May 2019.

19. Koros WJ, Zhang C. *Ultra-selective carbon molecular sieve membranes and methods of making.* United States patent. 15/170,529. 27 July 2016.

20. Bhave RR, Linneen NN. *Carbon molecular sieve membrane for gas separations*. United States patent 10758873 B2. 1 September 2020.

21. Hamm JBS, Ambrosi A, Griebeler JG, Marcilio NR, et al. Recent advances in the development of supported carbon membranes for gas separation. *International Journal of Hydrogen Energy*. 2017;42(39):24830-24845. DOI:10.1016/j.ijhydene.2017.08.071

22. Amirkhanov DM, Alekseeva OK, Kotenko AA, Kruchinina EV, et al. Analysis of the current state of processes for obtaining composite carbon gas-selective membranes formed under conditions of controlled carbonization of polymers. *Membrani.* 2006;4(32):19-39. (In Russ.)

23. Saufi SM, Ismail AF. Fabrication of carbon membranes for gas separation – a review. *Carbon*. 2004;42(2):241-259. DOI:10.1016/j.carbon.2003.10.022

24. Lei L, Pan F, Lindbråthen A, Zhang X, et al. Carbon hollow fiber membranes for a molecular sieve with precise-cutoff ultramicropores for superior hydrogen separation. *Nature Communications*. 2021;12(1):268. DOI:10.1038/s41467-020-20628-9

25. Zhang C, Kumar R, Koros WJ. Ultra-thin skin carbon hollow fiber membranes for sustainable molecular separations. *AIChE Journal*. 2019;65(8):e16611. DOI:10.1002/aic.16611

26. Haider S, Lie J, Lindbråthen A, Hägg M-B. Pilot–scale production of carbon hollow fiber membranes from regenerated cellulose precursor-part II: carbonization procedure. *Membranes*. 2018;8(4):97. DOI:10.3390/membranes8040097

27. Ghorpade RV, Lee S, Hong SC. Effect of different itaconic acid contents of poly(acrylonitrile-co-itaconic acid)s on their carbonization behaviors at elevated temperatures. *Polymer Degradation and Stability*. 2020; 181:109373. DOI:10.1016/j.polymdegradstab.2020.109373

28. Wu S, Gao A, Wang Y, Xu L. Modification of polyacrylonitrile stabilized fibers via post-thermal treatment in nitrogen prior to carbonization and its effect on the structure of carbon fibers. *Journal of Materials Science*. 2018;53(11):8627-8638. DOI:10.1007/s10853-017-1894-8

29. Gutmann P, Moosburger-Will J, Kurt S, Xu Y, et al. Carbonization of polyacrylonitrile-based fibers under defined tensile load: influence on shrinkage behavior, microstructure, and mechanical properties. *Polymer Degradation and Stability*. 2019;163:174-184. DOI:10.1016/j.polymdegradstab.2019.03.007

30. Saha B, Schatz GC. Carbonization in polyacrylonitrile (PAN) based carbon fibers studied by ReaxFF molecular dynamics simulations. *The Journal of Physical Chemistry B*. 2012;116(15):4684-4692. DOI:10.1021/jp300581b

31. Yushkin AA, Efimov MN, Vasilev AA, Bogdanova YuG, et al. Modification of polyacrylonitrile membranes by incoherent IR radiation. *Petroleum Chemistry*. 2017;57(4):341-346. DOI:10.1134/S0965544117040089

32. Yushkin AA, Efimov MN, Vasil'ev AA, Ivanov VI, et al. Effect of IR radiation on the properties of polyacrylonitrile and membranes on its basis. *Polymer Science, Series A*. 2017;59(6):880-890. DOI:10.1134/S0965545X17060104

33. Lee WH, Bae JY, Yushkin A, Efimov M, et al. Energy and time efficient infrared (IR) irradiation treatment for preparing thermally rearranged (TR) and carbon molecular sieve (CMS) membranes for gas separation. *Journal of Membrane Science*. 2020;613: 118477. DOI:10.1016/j.memsci.2020.118477

34. Renschler CL, Sylwester AP, Salgado LV. Carbon films from polyacrylonitrile. *Journal of Materials Research*. 1989;4(2):452-457. DOI:10.1557/JMR.1989.0452

35. Chernikova EV, Poteryaeva ZA, Shlyakhtin AV, Prokopov NI, et al. Effects of synthesis conditions and the mechanism of homopolymerization of acrylonitrile on the thermal behavior of the resulting polymer. *Polymer Science Series B*. 2013;55(1-2):1-13. DOI:10.1134/S1560090412110012

36. Yushkin AA, Efimov MN, Malakhov AO, Karpacheva GP, et al. Creation of highly stable porous polyacrylonitrile membranes using infrared heating. *Reactive and Functional Polymers*. 2021;158:104793. DOI:10.1016/j.reactfunctpolym.2020.104793

37. Devasia R, Nair CPR, Sadhana R, Babu NS, et al. Fourier transform infrared and wide-angle X-ray diffraction studies of the thermal cyclization reactions of high-molar-mass poly(acrylonitrile-*co*-itaconic acid). *Journal of Applied Polymer Science*. 2006;100(4):3055-3062. DOI:10.1002/app.23705

38. Matveev D, Vasilevsky V, Volkov V, Plisko T, et al. Fabrication of ultrafiltration membranes from non-toxic solvent dimethylsulfoxide: benchmarking of commercially available acrylonitrile co-polymers. *Journal of Environmental Chemical Engineering*. 2022;10(1): 107061. DOI:10.1016/j.jece.2021.107061

39. Ju A, Guang S, Xu H. Effect of comonomer structure on the stabilization and spinnability of polyacrylonitrile copolymers. *Carbon*. 2013;54:323-335. DOI:10.1016/j.carbon.2012.11.044

40. Ouyang Q, Cheng L, Wang H, Li K. Mechanism and kinetics of the stabilization reactions of itaconic acid-modified polyacrylonitrile. *Polymer Degradation and Stability*. 2008;93(8):1415-1421. DOI:10.1016/j.polymdegradstab.2008.05.021

41. McKelvey S. Phase separation, vitrification, and the manifestation of macrovoids in polymeric asymmetric membranes. *Journal of Membrane Science*. 1996;112(1): 29-39. DOI:10.1016/0376-7388(95)00197-2

42. Bildyukevich AV, Hliavitskaya TA, Nevar TN. Influence of spinning modes on the structure and properties of polyethersulfone hollow-fiber ultrafiltration membrane. *Membranes and Membrane Technologies*. 2022;4(4):195-205. DOI:10.1134/S2517751622040023

43. Bildyukevich AV, Plisko TV, Usosky VV. The formation of polysulfone hollow fiber membranes by the free fall spinning method. *Petroleum Chemistry*. 2016;56(5):379-400. DOI:10.1134/S0965544116050042

44. Kujawski W, Adamczak P, Narebska A. A fully automated system for the determination of pore size distribution in microfiltration and ultrafiltration membranes. *Separation Science and Technology*. 1989;24(7-8):495-506. DOI:10.1080/01496398908049787

45. Faraji S, Yardim MF, Can DS, Sarac AS. Characterization of polyacrylonitrile, poly(acrylonitrile-*co*-vinyl acetate), and poly(acrylonitrile-*co*-itaconic acid) based activated carbon nanofibers. *Journal of Applied Polymer Science*. 2017;134(2):app.44381. DOI:10.1002/app.44381

46. Araújo T, Parnell AJ, Bernardo G, Mendes A. Cellulose-based carbon membranes for gas separations – unraveling structural parameters and surface chemistry for superior separation performance. *Carbon*. 2023;204:398-410. DOI:10.1016/j.carbon.2022.12.062

47. Yushkin AA, Balynin AV, Nebesskaya AP, Chernikova EV, et al. Acrylonitrile-acrylic acid copolymer ultrafiltration membranes for selective asphaltene removal from crude oil. *Membranes*. 2023;13(9):775. DOI:10.3390/membranes13090775

48. Kim D, Kwon Y, Lee J-H, Kim S-J, et al. Tailoring the stabilization and pyrolysis processes of carbon molecular sieve membrane derived from polyacrylonitrile for ethylene/ethane separation. *Membranes*. 2022;12(1):93. DOI:10.3390/membranes12010093

49. Hameed N, Sharp J, Nunna S, Creighton C, et al. Structural transformation of polyacrylonitrile fibers during stabilization and low temperature carbonization. *Polymer Degradation and Stability*. 2016;128:39-45. DOI:10.1016/j.polymdegradstab.2016.02.029

Information about the authors / Информация об авторах

Ala L. Yaskevich, Cand. Sc. (Chem.), Leading Researcher, Institute of Physical Organic Chemistry, National Academy of Sciences of Belarus (IPOC), Minsk, Belarus; ORCID 0000-0003-4542-2680; e-mail: Yaskevich1909@gmail.com

Tatsiana A. Hliavitskaya, Cand. Sc. (Chem.), Leading Researcher, IPOC, Minsk, Belarus; ORCID 0000-0002-5236-7061; e-mail: thliavitskaya@gmail.com

Alexey A. Yushkin, Cand. Sc. (Chem.), Leading Researcher, A.V. Topchiev Institute of Petrochemical Synthesis, Russian Academy of Sciences (TIPS RAS), Moscow, Russian Federation; ORCID 0000-0002-0118-1515; e-mail: Halex@ips.ac.ru

Svetlana A. Pratsenko, Cand. Sc. (Chem.), Leading Researcher, IPOC, Minsk, Belarus; ORCID 0000-0002-6358-6251; e-mail: membrana@ifoch.bas-net.by

Evgenii A. Nazarov, Researcher, IPOC, Minsk, Belarus; e-mail: nazevgeny@gmail.com

Mikhail N. Efimov, Cand. Sc. (Chem.), Leading Researcher, TIPS RAS, Moscow, Russian Federation; ORCID 0000-0001-7996-474X; e-mail: efimov@ips.ac.ru

Dmitry G. Muratov, Cand. Sc. (Eng.), Leading Researcher, TIPS RAS, Moscow, Russian Federation; ORCID 0000-0002-4865-288X; e-mail: muratov@ips.ac.ru

Tatiana V. Plisko, Cand. Sc. (Chem.), Head of Laboratory, IPOC, Minsk, Belarus; ORCID 0000-0002-6534-7596; e-mail: plisko.v.tatiana@gmail.com

Alexandr V. Bildyukevich, D. Sc. (Chem), Academician, Director of IPOC, Minsk, Belarus; ORCID 0000-0003-3662-9970; e-mail: uf@ifoch.bas-net.by

Яскевич Ала Леонидовна, кандидат химических наук, старший научный сотрудник, Институт физико-органической химии Национальной академии наук Беларуси (ИФОХ НАН Беларуси), Минск, Республика Беларусь; ORCID 0000-0003-4542-2680; e-mail: Yaskevich1909@gmail.com

Глевицкая Татьяна Александровна, кандидат химических наук, старший научный сотрудник, ИФОХ НАН Беларуси, Минск, Республика Беларусь; ORCID 0000-0002-5236-7061; e-mail: thliavitskaya@gmail.com

Юшкин Алексей Александрович, кандидат химических наук, старший научный сотрудник лаборатории полимерных мембран, Институт нефтехимического синтеза им. А. В. Топчиева РАН (ИНХС РАН), Москва, Российская Федерация; ORCID 0000-0002-0118-1515; e-mail: Halex@ips.ac.ru

Праценко Светлана Анатольевна, кандидат химических наук, старший научный сотрудник, ИФОХ НАН Беларуси, Минск, Республика Беларусь; ORCID 0000-0002-6358-6251; e-mail: membrana@ifoch.bas-net.by

Назаров Евгений Артурович, младший научный сотрудник, ИФОХ НАН Беларуси, Минск, Республика Беларусь; e-mail: nazevgeny@gmail.com

Ефимов Михаил Николаевич, кандидат химических наук, ведущий научный сотрудник, ИНХС РАН, Москва, Российская Федерация; ORCID 0000-0001-7996-474X; e-mail: efimov@ips.ac.ru

Муратов Дмитрий Геннадьевич, кандидат технических наук**,** ведущий научный сотрудник, ИНХС РАН, Москва, Российская Федерация; ORCID 0000-0002-4865-288X; e-mail: muratov@ips.ac.ru

Плиско Татьяна Викторовна, кандидат химических наук, заведующий лабораторией, ИФОХ НАН Беларуси, Минск, Республика Беларусь; ORCID 0000-0002-6534-7596; e-mail: plisko.v.tatiana@gmail.com

Бильдюкевич Александр Викторович, доктор химических наук, академик, директор ИФОХ НАН Беларуси, Минск, Республика Беларусь; ORCID 0000-0003-3662-9970; e-mail: uf@ifoch.bas-net.by

Received 04 July 2024; Accepted 30 August 2024; Published 22 October 2024